Disponible en **www.hormigonyacero.com**
Hormigón y Acero 2024
https://doi.org/10.33586/hya.2023.3116

Questions on Shear Behavior of Structural Concrete and Answers Provided by Mechanical Models. The Challenge of Performance-Based Shear Design

Preguntas sobre comportamiento a cortante en hormigón estructural y respuestas aportadas por modelos mecánicos. El reto del proyecto a cortante basado en prestaciones

Antonio Marí [a*]

[a] *Professor. Department of Civil and Environmental Engineering Polytechnic University of Catalunya. Barcelona, Spain*

Recibido el 17 de noviembre de 2022; revisado el 19 de abril de 2023, aceptado el 20 de abril de 2023

ABSTRACT

The shear behavior and strength of reinforced and prestressed concrete structures are difficult to predict due to the complex resistant mechanisms that are mobilized and the different types of failure that can occur. This has given rise to many of the simplified formulations previously developed for shear calculation being empirical in nature, which lack a clear theoretical basis and they do not provide qualitative information on structural behavior. Therefore, performance-based design becomes difficult using such types of formulations. In this paper, some questions about shear behavior and design are raised, apparently without an immediate answer from the performance point of view, and possible answers based on structural mechanics are provided. The physical phenomena that determine the shear behavior, the resistant mechanisms that are developed, the fundamental parameters that govern them, to what extent they influence and how they are contemplated in some simplified formulations are analyzed. The importance of mechanical models is raised and some examples of how these models can be naturally adapted to multiple project situations, evaluation and reinforcement of existing structures are shown.

KEYWORDS: Shear, structure, strength, reinforced concrete, performance-based design, mechanical models, assessment.

RESUMEN

El comportamiento y la resistencia a esfuerzo cortante de estructuras de hormigón armado y pretensado resultan de difícil predicción por los complejos mecanismos resistentes que se movilizan y las distintas formas de rotura que pueden producirse. Ello ha dado lugar a que muchas de las formulaciones simplificadas previamente desarrolladas para cálculo a cortante sean de carácter empírico, sin un claro fundamento teórico y no proporcionen información cualitativa sobre comportamiento estructural, lo que dificulta el proyecto basado en prestaciones. En este artículo se plantean algunas preguntas sobre diseño y comportamiento a cortante, aparentemente sin una respuesta lógica desde el punto de vista prestacional, y se aportan posibles respuestas basadas en la mecánica estructural. Se analizan los fenómenos físicos que determinan el comportamiento a cortante, los mecanismos resistentes que se desarrollan, los parámetros fundamentales que los gobiernan, en qué medida influyen y como son contemplados en algunas formulaciones simplificadas. Se plantea la importancia de los modelos mecánicos y se muestran algunos ejemplos de cómo estos modelos pueden adaptarse de forma natural a múltiples situaciones de proyecto, evaluación y refuerzo de estructuras existentes.

PALABRAS CLAVE: Cortante, estructuras, resistencia, hormigón armado, proyecto basado en prestaciones, modelos mecánicos, evaluación.

* Persona de contacto / *Corresponding author*:
Correo-e / *e-mail*: antonio.mari@upc.edu (Antonio Marí)

How to cite this article: Marí, A. (2024) Questions on Shear Behavior of Structural Concrete and Answers Provided by Mechanical Models. The Challenge of Performance-Based Shear Design, *Hormigón y Acero* 75(302-303): 7-24. https://doi.org/10.33586/hya.2023.3116

NOTATION

a	shear span,
b	width of the cross-section.
$b_{v,eff}$	effective width of T shaped cross sections for shear strength
b_w	width of the web on T, I or L beams. For rectangular beams $b_w = b$
d	effective depth of the cross-section.
d_0	effective depth of the cross-section, d, but not less than 100 mm
f_{cc}	concrete compressive strength, in general
f_{cd}	design value of concrete compressive strength
f_{ck}	characteristic compressive strength of concrete

f_{cm} mean compressive strength of concrete
f_{ct} concrete tensile strength, in general
f_{ctm} mean tensile strength of concrete, in MPa
f_{ywd} design yield strength of the shear reinforcement
h overall depth of a cross-section
h_f height of the compression flange in T, I or L beams.
s distance from the considered section to the point of zero bending moment
s_t spacing of the stirrups
s_{cr} location of the section where the critical shear crack starts
x neutral axis depth of the cracked section
x_0 neutral axis depth of a PC member considering P = 0
y vertical coordinate in section analysis
z inner lever arm corresponding to the bending moment
A_c area of concrete cross section
A_s area of mild reinforcement
A_{sw} cross-sectional area of the shear reinforcement
$A_{sw,min}$ minimum cross sectional area of shear reinforcement
E_s modulus of elasticity of reinforcing steel
K_{ad} shear strength amplification factor in non-slender beams
K_c is equal to the relative neutral axis depth, x/d, but not greater than 0.20
K_τ shear stresses integration constant
M_{cr} cracking moment at the section where shear strength is checked
M_E concomitant bending moment
N_E concomitant axial or prestressing force
P prestressing force after total losses
V_{cu} contribution of the concrete to the shear strength of a member
V_{Ed} design shear force in the section considered
V_{Rd} design shear resistance of the member
$V_{Rd,max}$ design value of the maximum shear force which can be sustained by the member
V_{su} contribution of the shear reinforcement to the shear strength of a member
V_u Shear strength computed according to a theoretical model
α angle between shear reinforcement and the longitudinal beam axis
α_{cw} coefficient taking account the state of the stress in the struts
α_E modular ratio, $\alpha_E = E_s/E_{cm}$
υ_1 strength reduction factor for concrete cracked in shear
θ angle between the concrete compression strut and the beam longitudinal axis
ρ_l longitudinal tensile reinforcement ratio referred to the effective depth d and the width b.
σ_{cp} concrete compressive stress at the centroidal axis due to axial loading and/or prestressing
σ_x concrete normal stress, in the longitudinal x axis
σ_y concrete normal stress, in the vertical y axis
σ_1 concrete principal tensile stress
σ_2 concrete principal compressive stress
τ concrete shear stress
ζ size effect factor

1. INTRODUCTION

The current trend in structural design codes is to allow the designer, under his/her responsibility, to adopt hypotheses or use design equations, based on theoretical principles or test results, other than those proposed or explicitly accepted in the code, provided that the required levels of safety, functionality and durability are satisfied. This is called "Performance-based design (PBD)" and, in order to carry out such type of design, it is necessary to clearly understand the structural behavior, to identify the variables that govern it and to what extent they do so, among other aspects.

In the case of shear design, the phenomena that take place are of considerable complexity and it is not immediate to take them into account in formulations intended for design, which must necessarily be simple and at the same time capture the most important phenomena with a certain degree of conservatism. For this reason, in many design codes, empirical formulas developed adjusting mathematical functions to experimental results, have been often adopted. Despite being a good approach in design phases, these formulas are essentially a black box in unforeseen situations, what is an important limitation for performance-based design.

Numerical methods are currently available that rigorously simulate the complex phenomena affecting the shear behavior and strength. However, despite the enormous advances made in this field, they are still limited in engineering practice to particular cases or for research tasks, where they can help to verify some hypothesis or may be used as simulators of physical experiments, in order to perform parametric studies.

In between empirical and numerical models are the mechanical models, based on the principles of the structural mechanics of reinforced concrete, that try to capture the experimentally observed behavior. The best-known case is that of the Ritter and Mörsch truss analogy [1], [2] which simulates the behavior of a reinforced beam cracked in shear by means of a system of distributed struts and ties, in equilibrium with external loads. Although there are some aspects of shear behavior not considered in this model, it has been the basis of the shear design methods for beams with shear reinforcement for more than a century, thanks to its mechanical nature.

Because of their genesis, mechanical models provide an insight into the physics of the problem and allow expressions to be derived, in which the governing parameters of the shear behavior appear naturally with its corresponding weight. In addition, they allow to capture contributions or aspects usually not accounted for in the design phase, but which may be relevant in the evaluation of existing structures. The ability to adequately capture the influence of the different parameters allows for justifiable simplifications, limiting the errors made. As a result, formulations can be derived that are sufficiently simple but accurate at the same time, to serve in the design stage of new structures, and for evaluation and strengthening of existing structures. Moreover, its extrapolation or adaptation to new situations of geometry, materials or loads, is straightforward by accounting for the differential aspects of the case under study.

This paper aims to show how mechanical models may contribute to the understanding of some aspects of the shear behavior and strength of structural concrete members. For this purpose, the most relevant phenomena affecting the shear behavior, the shear transfer actions developed and the behavior under increasing load up to failure are briefly described. Next, a classification of the mechanical models is made based on how they address the previously mentioned aspects, emphasizing on those methods based on the contribution of the uncracked compression chord as main shear transfer action. A series of questions about aspects of shear behavior and design often not sufficiently well understood, are posed and possible answers are given, based on how the "Multi-action Shear Model" (MASM) [3], [4] and its simplification, the "Compression Chord Capacity Model" (CCCM) [5] face the shear design. Subsequently, in order to demonstrate the accuracy and robustness of these mechanical models, comparisons between their predictions with the results of 3295 shear tests on a large variety of members with different geometry, reinforcement arrangements, types of loading and materials, are made.

2. RELEVANT ASPECTS OF THE SHEAR BEHAVIOR OF CONCRETE STRUCTURES

The complexity of the shear behavior of reinforced and prestressed concrete structures can be associated to the low tensile strength of concrete, to the presence of combined normal and shear stresses and to the quasi-brittle nature of concrete. Consequences of these phenomena are, among others:

- The inclination of the principal stresses, and thus, the formation of diagonal cracks, which deeply modify the stresses fields and the flow of forces in the concrete (cracking-induced anisotropy), and give place to the so-called shear-flexure interaction.
- The influence of the multiaxial state of stresses on concrete strength. As a consequence, the verification of the concrete strength using the uniaxial compressive strength (adopted in design) must be reduced or enhanced as a function of the orthogonal principal stress, as it occurs in concrete struts but also in uncracked concrete zones. Such effect can be quantified through biaxial failure envelopes.
- The reduction of the mean shear stress, τ_m , resisted by a beam, $\tau_m = V/(bd)$, as the beam dimensions increase, known as "size effect". A transition from nearly ductile behavior in small concrete structures to nearly brittle behavior in large ones takes place due to the material heterogeneity which causes the fracture process zone to be long and non-negligible compared to the cross-section size.
- The enhancement of the shear strength of a beam as the ratio between the shear span and the effective depth decreases, as it occurs in deep beams and in beams subjected to concentrated loads applied near the supports. In those cases, the lower value of a/d, the higher the shear that can be resisted
- The favorable effects of the confinement introduced by stirrups in the concrete compressed chord, producing on it a multi-axial state stress. Likewise, the transverse reinforcements contribute to reducing the risk of failure due to sliding in inclined cracks.
- The possible spalling of the concrete cover, longitudinal cracking and loss of anchorage of the longitudinal reinforcement in members subjected to strong shear forces, in which high bond stresses are produced due to the variation of its tensile force in longitudinal bars.

The aforementioned phenomena are accounted for, to a greater or lesser extent, through different shear resistant mechanisms. According to ASCE-ACI Committee 445 [6], the shear strength in a RC beam is provided by the following contributions (see Figure 1):

- The shear resisted by the un-cracked concrete chord V_c , which is subjected to normal and shear stresses due to shear forces, axial forces and bending moments. The maximum shear force resisted is associated to the state of principal stresses that reaches a point of the concrete biaxial failure envelope.
- The shear transferred along the cracks, V_w, which is composed by the residual stresses that can be transferred across the crack and by the force transferred through aggregate interlock.
- The shear resisted directly by the transverse reinforcement, V_s, crossing the critical crack
- The shear resisted by the longitudinal reinforcement, V_l, subjected to differential displacements of the two opposite faces of the inclined crack, called dowel action.

In general, the four above mentioned main shear transfer actions are grouped into two, called the concrete contribution V_{cu}, considered as the sum of V_c, V_w and V_l and the steel contribution Vsu:

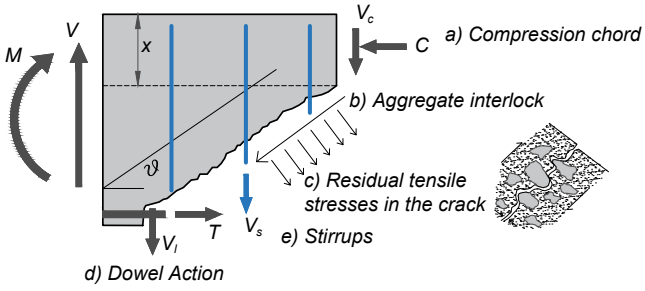

Figure 1. Shear transfer actions

There is a general consensus in the value of V_s, that can be derived from the well-known truss model. However, there are relevant differences in the value assigned to the concrete contribution V_c in different codes of practice, as the relative contribution of each shear transfer action may change along the loading process due to cracking and softening of concrete under multiaxial state of stresses, yielding of the reinforcement, bond slip and other nonlinear phenomena.

As the load increases, localization of damage takes place and concentrates in a critical crack, whose width increases; hence, shear transferred by aggregate interlock and the residual stresses crossing the crack tend to reduce. Then, shear stresses concentrate around the neutral axis, and enter into the uncracked concrete chord, that will be subjected to a multiaxial stress state consisting of at least normal compression and shear stresses.

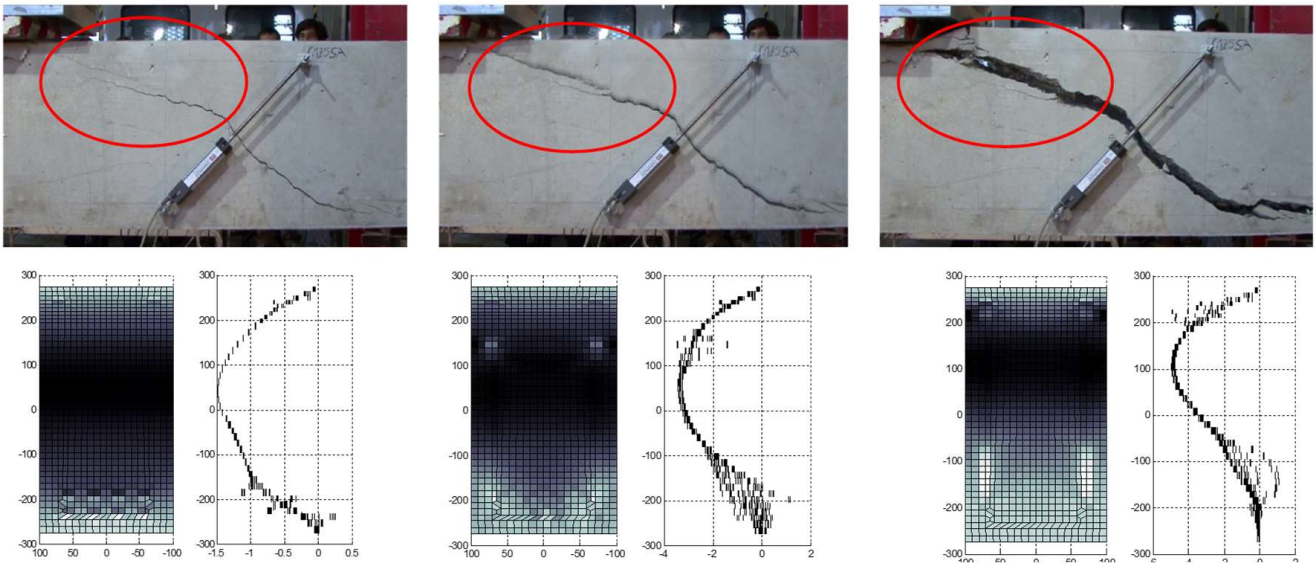

Figure 2. Evolution of cracking and shear stresses in a beam without shear reinforcement [7].

Figure 3. Shear web failures. Left: diagonal tension. Right: by web struts crushing [10].

Eventually, a second branch of the critical crack develops above the neutral axis trough the compression chord, in the point that first reaches the concrete strength under multiaxial stresses state, initiating softening of its shear transfer capacity.

Figure 2 shows the typical evolution of the shear stresses in a reinforced concrete section, in the elastic, cracked and ultimate stages under increasing loading driving to a shear-flexural- failure, obtained through computer program Total Interaction Nonlinear Sectional Analysis (TINSA), developed by Bairán [7].

At the same time, tensile shift in the longitudinal reinforcement increases, which may produce bond cracks in the bottom reinforcement. If premature bond failure does not take place, failure of the element will be controlled by the shear capacity of the compression chord as it is the last element that typically initiates softening. A detailed analysis of the shear transfer actions in reinforced concrete was done by Cavagnis *et al.* [8], using Digital Image Correlation. Bairán *et al.* [9] also performed an analysis of the shear resisting actions by means of optimization of strut and tie models according to crack patterns.

Other types of failure can take place, such as it occurs in prestressed pretensioned members without or with very low shear reinforcement ratio, in regions without flexural cracks. In those cases, failure usually occurs when the principal stresses at a point in the web reach the strength of the concrete under the biaxial state of stress (Figure 3.a). A diagonal crack is generated in the web that extends towards the tension and compression heads.

Finally, in elements with high amount of shear reinforcement, and thin webs, failure may occur due to excessive compression in the compressed struts (Figure 3, right).

3. BRIEF DESCRIPTION OF SOME SELECTED MECHANICAL SHEAR MODELS

A number of available mechanical models, grouped according to the assumptions made, to the shear transfer mechanism considered dominant and to the way the size effect is treated, are briefly described. Among the many existing models, for the sake of simplicity and space, only a selected number of them are mentioned next

3.1. Models based on aggregate interlock, theory of plasticity or fracture mechanics

The Modified Compression Field Theory (MCFT), developed by Vecchio and Collins in 1986 [11], is a general model for

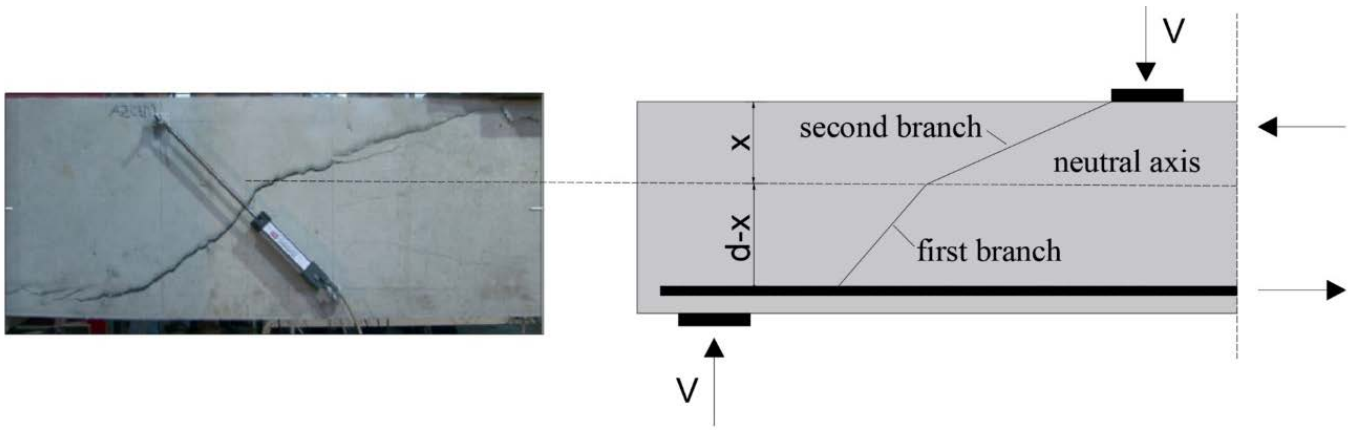

Figure 4. Assumed shape of the critical shear crack.

bidimensional elements subjected to shear and normal stresses. The equilibrium equations, the compatibility conditions, and the constitutive equations of cracked concrete and reinforcement enable to obtain, through an iterative process, the average stress, the average strain and the angle θ of inclination of the cracks for any load level up to failure. Failure of the RC element is rather governed by the local stresses occurring at a crack. This method was adopted by the Canadian code CSA (1994) [12] and the AASHTO (2000) [13], after some modifications made by Bentz *et al* [12].

The Critical Shear Crack Theory, (CSCT), by Muttoni and Fernández-Ruiz [15] assumes that the shear strength of members without stirrups is considered to be strongly dependent on the critical shear crack width (which is considered proportional to the longitudinal strain at a distance 0.6d of the most compressed fiber, in a defined critical section), and on its roughness. The maximum aggregate size is an explicit parameter affecting the reduction of shear capacity due to size effect [16]. After some modifications this method was included as part of the Model Code 2010 provisions [17].

The Critical Shear Displacement Model developed by Yang, Walraven and Ujil [18], propose that the unstable opening of the critical inclined crack is triggered when the shear displacement in an existing flexural crack reaches a critical value Δ_{cr}. Thus the critical shear displacement is used as a failure criterion, and based on that a new shear evaluation method was proposed.

The above-mentioned models adopt the previous works made by Walraven [19] in 1981, to estimate the shear stresses along shear cracks.

Based on the Theory of Plasticity, Nielsen [20], stated in 1984 that once the stirrups yield, increasing shear force can only be carried by increasing the compression stress σ_c which at the same time rotates to smaller angles θ. According to this theory, shear failure occurs either due to yielding of the stirrups or crushing of concrete in the web of the element. Direct applications of the Theory of plasticity iare the Strut and Tie Method, Schalich *et al.* [21] and the variable angle strut method adopted by Eurocode EC2 [22], both for D regions and for B regions, assuming that no contribution of concrete exists. Reineck [23] proposed a method based on the Strut and Tie models applicable to beams without stirrups, considering that the concrete ties represent the shear resisting actions developed in the beam after diagonal cracking.

Bazant and Kim [24] developed a model considering concrete as a quasi-brittle material, since it possesses a large fracture process zone relative to its crack size. They proposed a structural size effect law to describe the quasi-brittle nature of concrete according to non-linear fracture mechanics, which captures the transition from the results obtained using Linear Elastic Fracture Mechanics (LEFM) and a plastic size criterion. This size effect model has been adopted in the last version of the ACI 318-19 [25], [26]. Another well-known model based on non-linear fracture mechanics is the Fictitious Crack Model, developed by Hillerborg [27]. Recently, Carmona and Ruiz [28] studied through fracture mechanics the influence of bond between the reinforcing bars and the concrete matrix and the size effect on the evaluation of shear strength in reinforced concrete members without stirrups.

3.2. Models based on the contribution of the uncracked concrete chord

A number of developed models consider the contribution of the compression chord as the main shear transfer action. In general, models based on this approach assume that in slender beams without shear reinforcement under two-point loading, the critical shear crack typically involves two branches, (Figure 4). The opening of the first branch of the critical crack is assumed to be orthogonal to the line of the crack, being the result of a rotation around its tip. The compression zone above the tip prevents any meaningful contribution of shear slip along the crack interface, thus the contribution of aggregate interlock and dowel action are considered small and may be neglected.

Some of the numerous relevant works done in this field are those of Kostovos *et al.* [29], Zararis and Papadakis [30], Tureyen and Frosch [31] and Park *et al.* [32], Li *et al* [33].

Recently, Marí *et al.* [3], [4], proposed the Multi-action Shear Model (MASM), which provides expressions for the contributions of the four shear transfer actions (V_u=V_c+V_w+V_l+V_s). As some models previously explained, the MASM considers that the uncracked concrete in flexure is subjected to a multiaxial state of principal stresses (σ_1, σ_2), generated by shear force (τ), longitudinal bending stresses (σ_x) and vertical stresses, (σ_y) due to local effects, that enhance the shear strength of the region. The effect of the confinement stresses in the uncracked concrete produced by the stirrups is incorporated to V_c.

A simplification of the MASM, is the Compression Chord Capacity Model (CCCM) developed by Cladera *et al* [5] in which the terms V_w and V_l, which according to the assumptions made in [3] are considered much lower than V_c, are incorporated into the contribution of the uncracked concrete chord, V_c, resulting in a much simpler formulation. In addition, a new size effect factor was introduced according to Bazant's law, modified after an empirical work performed with genetic programming in [34], to account for the shear slenderness a/d.

4. DERIVED EQUATIONS OF THE COMPRESSION CHORD CAPACITY MODEL

The most relevant assumptions of the CCCM made are:

- The shear stresses are concentrated in the uncracked compression chord, concrete tensile strength is neglected and the normal compressive concrete stresses distribution is linear.
- The critical shear crack starts at a section where at shear failure, the bending moment reaches the cracking moment of the section.
- The horizontal projection of the critical shear crack is 0.85d, based on experimental observations.
- The weakest section subjected to a combined shear-bending failure is considered to be located at the tip of the first branch of the critical crack, where it reaches the flexural neutral axis
- Failure is assumed to take place when the pair of principal stresses reach the Kupfer's Biaxial Failure Envelope, Figure 15, [35]
- For usual values of *a/d=M/Vd*, the critical point inside the compression chord, is located at a vertical distance from the neutral axis z=0.425x , being "x" the neutral axis depth.

The key equation to obtain the contribution of the concrete chord V_c, is the following:

$$V_c = \int_0^c \tau(y) b(y) dy = K_\tau \zeta x \sigma_1 \sqrt{1 - \frac{\sigma_x + \sigma_y}{\sigma_1} + \frac{\sigma_x \sigma_y}{\sigma_1^2}} \quad (1)$$

where

- $\tau(z)$ is the shear stress at a point of the uncracked chord at a distance "z" of the neutral axis,
- x is the neutral axis depth
- σ_1 is the principal tensile stress
- σ_x is the normal longitudinal stress due to bending
- σ_y is the normal vertical stress, if it exists
- K_τ is an integration constant
- ζ is the size effect factor given by Equation 6 of Table 1

Relating the normal stresses with the internal forces, and setting the equilibrium conditions Eq. (1) can be expressed as a function of the internal forces and the components of the shear transfer actions. Once solved, Eq. (1) provides a solution in which the contribution V_c is almost a linear function of x/d. Table 1 shows the main equations governing the shear strength for the CCCM, for beams with rectangular cross section. Note that V_{cu}, given by Eq. (4) includes, in addition to the compression chord contribution given by Eq. (6), the contributions of the shear actions V_w and V_l.

TABLE 1.
Summary of the CCCM equations for beam with rectangular cross section .

Equations	Expressions	
Shear strength	$V_{Rd} = V_{cu} + V_{su} \leq V_{Rd,max}$	(2)
Strut crushing	$V_{Rd,max} = \alpha_{cw} b_w z \nu_1 f_c \frac{cot\theta + cot\theta}{1 + cot^2\theta}$	(3)
Concrete contribution	$V_{cu} = \zeta \frac{x}{d} f_c^{2/3} b\, d \nleq V_{cu,min} = 0.25(\zeta K_c \frac{20}{d_0}) f_c^{2/3} bd$	(4)
Shear reinforcement	$V_{su} = 1.4 \frac{A_{sw}}{s_i} f_{yw} (d - x)\, sin\alpha (cot\theta + cot\alpha)$	(5)
Factors	**Expressions**	
Size and slenderness effect	$\zeta = \frac{2}{\sqrt{1 + \frac{d_0}{200}}} \left(\frac{d}{a}\right)^{0.2} \nleq 0.45$	(6)
Relative neutral axis depth	$\frac{x}{d} = \alpha_E \rho_l \left(-1 + \sqrt{1 + \frac{2}{\alpha_E \rho_l}}\right) \approx 0.75 (\alpha_E \rho_l)^{1/3}$	(7)
Crack inclination	$cot\theta = \frac{0.85\, d}{d - x} \leq 2.5$	(8)

Equations included in Table 1 are intended for design purposes, so they are expressed in terms of the design values of the materials strengths (f_{cd}, f_{ywd}), which incorporate the materials safety coefficients. However, when studying the structural behavior or when predicting tests results, mean values of the materials should be used. Furthermore, it must be pointed out that in the particular case of V_{cu}, Eq (4), V_{cu} was originally expressed in terms of the concrete mean tensile strength, fctm, (see reference [3] and section 5.8), as follows

$$V_{cu} = \zeta \frac{x}{d} f_{ctm} bd \nleq V_{cu,min} = 0.83 (\zeta K_c + \frac{20}{d_0} f_{ctm} bd) \quad (9)$$

In the rest of the article, behavioral aspects will be addressed, so the written equations will not include safety coefficients.

The shear directly resisted by the shear reinforcement, given by Eq. (5), was derived considering the summation of the vertical force provided by the stirrups intersected by the first branch of the critical crack. The constant 1.4 in Eq. 5 is not a calibration factor, but a term to take into account the confinement of the concrete in the compression chord caused by the stirrups [3].

It should be noted that no iterations are needed to apply the model both for design or for assessment, since Eq. (4) is the linear solution adjusted to the actual solution of Eq. (1), once solved iteratively.

An example of shear design of a 2-span continuous shoring beam subjected to two concentrated loads at midspan is presented in Annex A1, which can help to better understand the method and the answers given to the questions raised below.

5. SOME QUESTIONS ON SHEAR BEHAVIOR OR DESIGN AND ANSWERS PROVIDED BY THE CCCM MECHANICAL MODEL

5.1. Why and how much the flexural reinforcement influences the shear strength?

According to CCCM, the shear strength contribution of the concrete chord is the result of the shear stresses in it, which depends on the depth of the compressed block, whose value is given by equation (7) of Table 1. It can be seen that x/d depends on the $\alpha_E \rho_l$ term, where $\rho = A_s/(bd)$ is the geometric

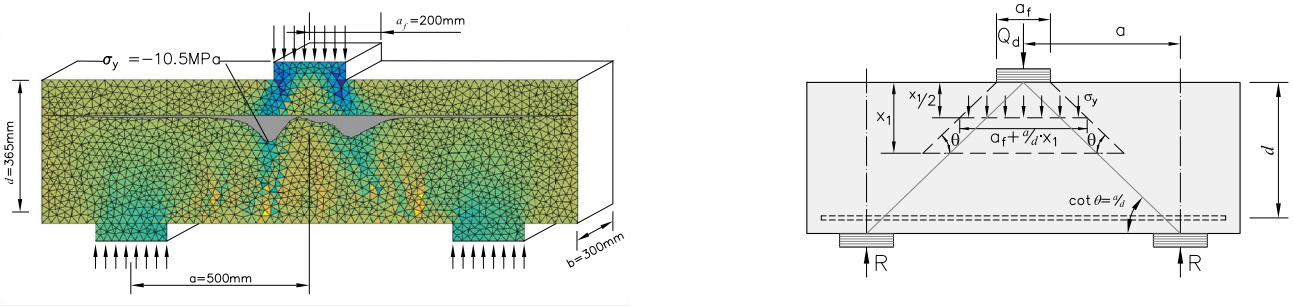

Figure 5. Vertical confining stresses in beams with loads applied near the supports [36].

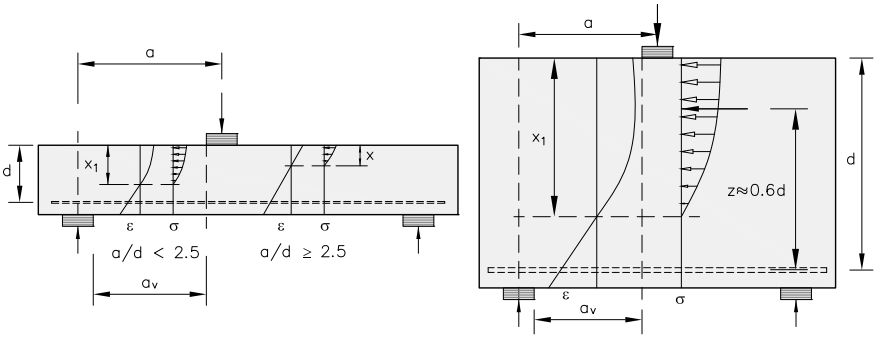

Figure 6. Distributions of stresses and strains in a slender and non-slender beam [36].

amount of longitudinal reinforcement and $\alpha_E = E_s/E_c$ is the ratio between the Moduli of elasticity of steel, E_s, and concrete, E_c, In addition to V_c, both V_l and V_w increase as the amount of longitudinal reinforcement increases, reducing the crack opening and incrementing the dowel action.

In addition, the angle of inclination of the cracks, given by the expression (8) depends also on x/d and, therefore on $\alpha_E\rho_l$. As can be seen, the greater the amount of reinforcement, the greater the cotθ, so the greater the number of stirrups cut by the critical crack and the greater the V_{su}, as indicated by equation (5). The same conclusion is drawn from the MCFT, and from the simplified equations adopted by the Canadian Standard for the angle of inclination of the cracks.

5.2. Why the shear slenderness "a/d" influences the shear strength?

The shear slenderness a/d is a relevant parameter because it influences the stress state of the concrete in the area where shear failure usually occurs

Non-slender beams are considered those in which a/d is less than 2.5 This situation takes place 1) in deep beams, where arch effect takes place due to the inclination of the compressed chord, 2) in slender beams when there are point loads applied near the supports and confining stresses under the loading plate may enhance the strength of the compression chord. As a consequence, non-slender beams show higher shear strength than slender beams.

How does the CCCM account for these effects?. The following differential aspects of the observed structural behavior are taken in consideration:

a) the influence of the vertical stresses produced by the loading plate, on the stress state in the critical point of the uncracked concrete chord. Such confining stresses, in the case of loads close to the supports, affect the state of stresses at the critical section) and increment the shear capacity of the compression chord, Figure 5, Bairán *et al.* [36]
b) the different position and inclination of the critical crack, which due to be located in a disturbed (D) region, runs straight from the inner ends of the bearing and loading plates, resulting in a value cotθ = *a/d*, see Figure 6. Such value increments the size effect factor of the model (Eq. 6), which is proportional to $(d/a)^{0.2}$;

Solving the fundamental equation (1) for some estimated average value of the vertical stresses, σ_y, see Figure 5, [32], the following expression for the contribution of the uncracked chord under point loads applied near the supports, is obtained as a function of σ_y:

$$V_c = \zeta \frac{x}{d} f_{ct} b d \left(1 + 0.5 \frac{\sigma_y}{f_{ct}}\right) \quad (10)$$

c) the effects of the disturbed distribution of strains and stresses in deep beams or in beams subjected to concentrated loads applied close to the support, which are not planar and modifies the neutral axis depth compared to a slender beam, see Figure 6.

In order to account for the increment of the neutral axis depth as the considered section approaches the support, a parabolic variation of *c* is assumed between *a/d* =2.5 (x_l=*x*, B-region) and *a/d*=0 (x_l=*d*) as follows:

$$\frac{x_1}{d} = \frac{x}{d} + \left(1 - \frac{x}{d}\right)\left(1 - 0.4 \frac{a}{d}\right)^2 \leq 1 \quad (11)$$

As a consequence of these assumptions, the concrete contribution of the uncracked chord, Vcu increases and can be expressed as

$$V_{cu} = \zeta \frac{x}{d} K_{ad} f_{ct} b d \cong 0.3 \xi K_{ad} f_c^{2/3} b d \quad (12)$$

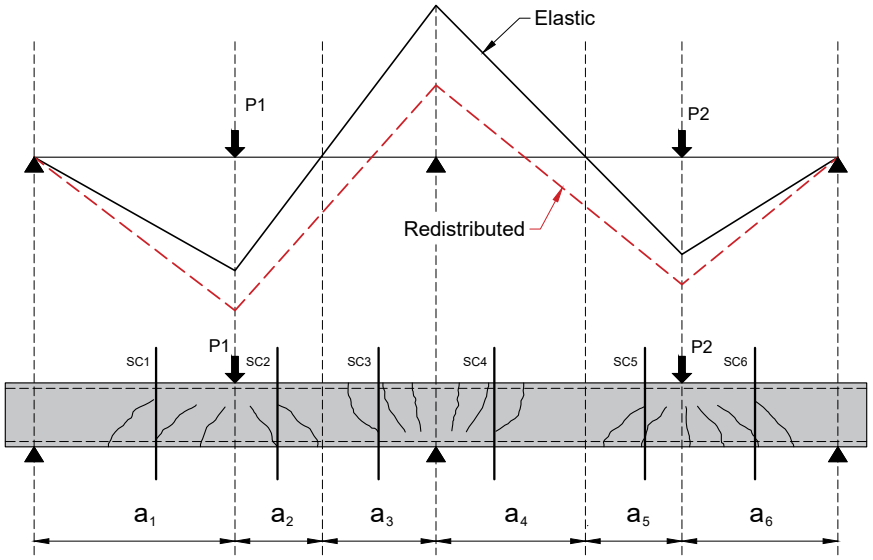

Figure 7. Bending moments law and crack patterns in a two-span RC continuous beam.

Where Kad is the factor enhancing the concrete contribution:

$$K_{ad}=1+(2.5-\frac{a}{d})^2 \;;\; 1\le \frac{a}{d} \le 2.5 \qquad (13)$$

5.3. *Do we distinguish between end supports and intermediate supports when designing a continuous beam for shear?*

In continuous beams, the same equations are used for shear design of the zones near the exterior supports (where very low bending moment exists) and near interior supports (with high load bending moments). Therefore, the presence of a bending moment concomitant with the shear force is not explicitly considered.

However, there are aspects of the structural behavior of continuous beams, usually not included in the codes of practice, that may justify such procedure

5.3.1. *Effects of the different shear spans in the various shear critical regions*

Figure 7 shows the law of bending moments and an approximate diagram of cracking in a continuous beam with two unequal spans, subjected to a point load in the respective spans.

It can be seen that there are three pairs of critical zones with similar behavior, where shear failure can occur: zones a1 and a6, near the end supports, zones a_2 and a_5 between the applied load and the zero bending moment point, and zones a_3 and a_4 around the central support.

As the respective shear spans (the distances from the point of application of the load or reaction to the point of zero moment), at each region the shear strength will also be different. In general, regions a_3 and a_4 have the shorter shear span, and the closer is the applied concentrated load to the support, the smaller is the shear span in such region. Therefore, it is expected that in the central support the shear span is lower than in the zone of positive bending moments and be even $a/d<2.5$.

5.3.2. *Effect of yielding of the longitudinal flexural reinforcement on the shear strength*

If the longitudinal flexural reinforcement yields in the zones of maximum negative moment, plastic hinges are formed and redistributions of bending moments and shear forces take place, as shown in Figure 7. Then, the point of zero bending moment becomes closer to the intermediate support, reducing the shear span and even increasing the arch effect (and the shear strength) in that area. Thus, since the design shear force decreases and the shear strength increases, the risk of shear-flexural failure around the central support diminishes.

Does the yielding of the flexural reinforcement reduce the shear capacity in the plastic hinge?. Once the reinforcement yields, its tensile force is limited to $T=A_s \cdot f_{yd}$ and so is the compression force. Therefore, as the load and the plastic rotation increase, the depth of the compressed block decreases, because it is necessary to increment the lever arm, and the width of the critical crack increases, so the contribution of the concrete decreases. Therefore, it is possible that in beams with very ductile sections, shear failure occurs inside the plastic hinge, before a collapse mechanism is formed. This type of shear-bending interaction has been experimentally studied by Vaz *et al.* [37] for simply supported beams and by Montserrat *et al.* [38], [39] for continuous beams.

5.3.3. *Effect of local stresses due to point loads or reactions*

In zones a1 and a6 of Figure 7, subjected to positive moments, the critical crack usually occurs at a sufficiently long distance from the load so that the vertical stresses produced by the load do not affect the state of stresses in the compression chord of the critical section.

However, in the hogging zones of Figure 7 (a_2, a_3, a_4 and a_5), the critical cracks develop near the application of the load or the support reaction, and compression stresses both in the longitudinal and the vertical directions take place in the compression chord, produced by the bending moment and by the applied load or reaction, respectively. These vertical stresses increase the shear strength in this zone, (see section 6.2), similarly to what occurs in punching shear around a column, Marí *et al.* [40]

In order to quantify such confining stresses, a two-span continuous beam loaded with two equal concentrated loads at midspan tested by Bagge el al. [41], Figure 8, has been studied, by means of a nonlinear analysis performed with software Diana [42].

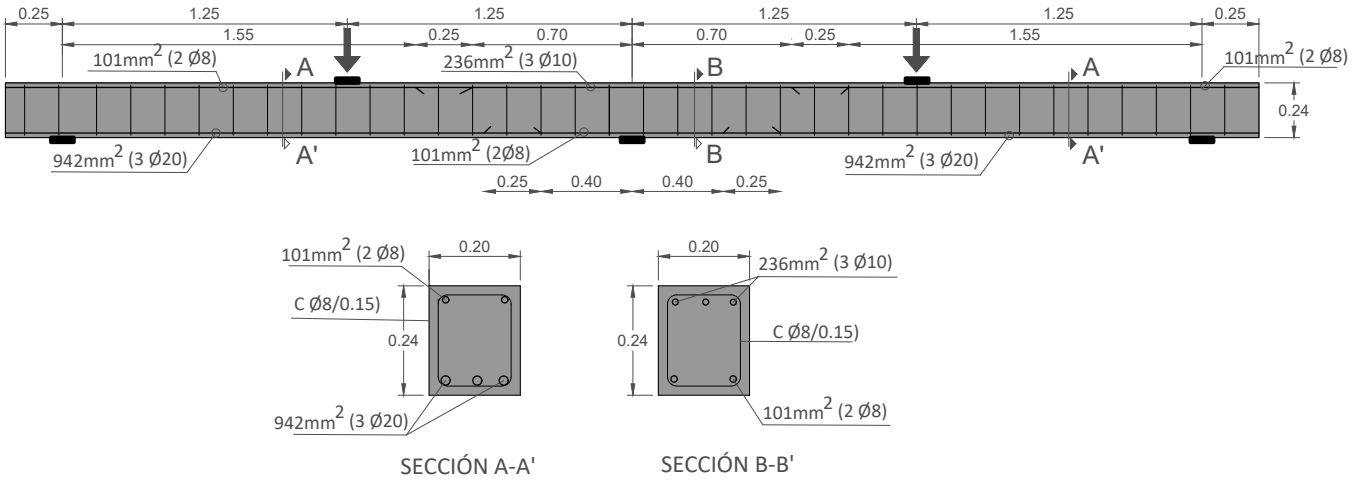

Figure 8. Scheme of the beams tested by Bagge *et al.* [41].

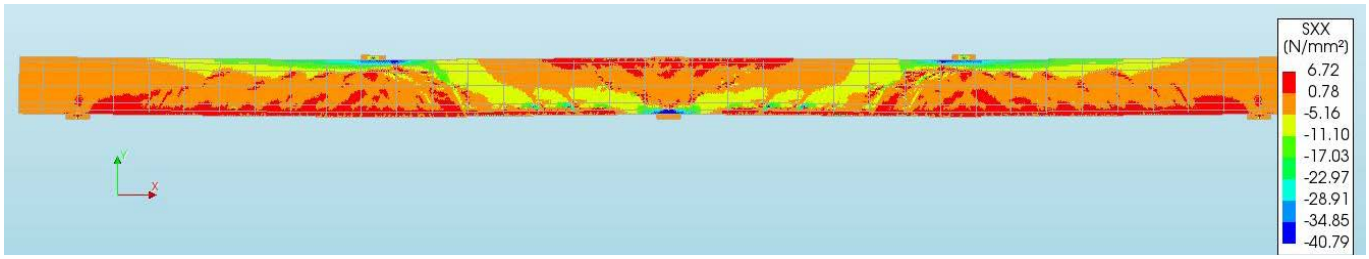

Figure 9a. Normal longitudinal stresses around the central support, near failure.

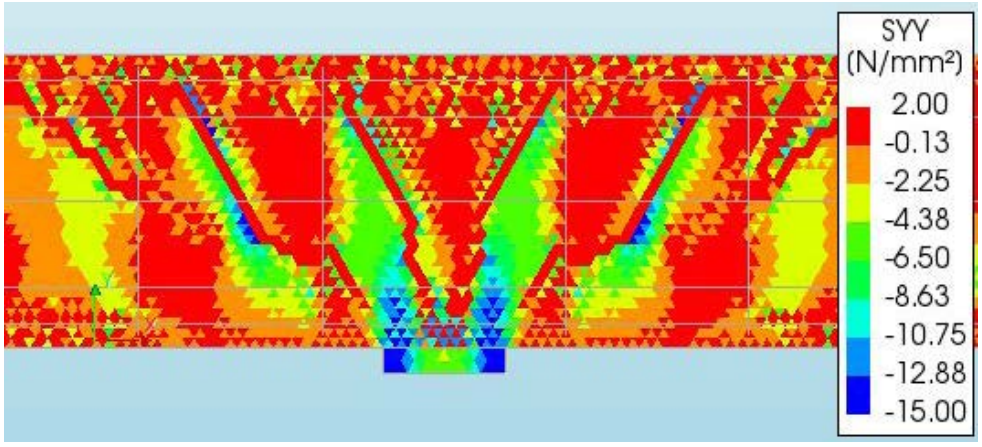

Figure 9b. Normal vertical stresses around the central support, near failure.

The reinforcement and the materials properties of the analyzed beam are: A_{s1}=339mm² (3ϕ12); A_{s2}=A_{s3}=101 mm² (2ϕ8) ; A_{s4}=942 mm² (3ϕ20) ; A_{sw}=0.67 mm²/mm (ϕ8, st=150 mm). f_{cm}=36.4 MPa, f_{yl}=536 MPa; f_{yw}=657 MPa.

Figures 9a and 9b show the normal longitudinal stresses along the whole beam and the vertical normal stresses localized around the central support, respectively.

It can be observed that near the position of the critical point (around mid-height of the compression chord) vertical stresses between 6 and 8 MPa and horizontal stresses in compression chord up to 12-25 MPa take place. According to equation 13, being f_c=34.6 MPa and f_{ct}=3.2 MPa, the increment of shear resisted by the concrete in the bottom of the section, due to confinement stresses, around the central support is 93 %. The ultimate load experimentally measured was 164 kN while the theoretical studies according to CCCM is 171 kN, which is 4.2% higher. This could explain why, in usual practice, the transverse reinforcement in the areas of intermediate supports, where negative moments are combined with shear forces, is designed in the same way as in extreme supports, where there is almost no bending moment, without shear resistance problems being revealed.

5.4. Why cantilevers resist more shear than identical simply supported beams.? Why cantilevers subjected to distributed load resist more shear than cantilevers subjected to point loads

Perez Caldentey *et al.* [43] tested reinforced concrete slender cantilevers with prismatic and tapered shapes, subjected to point loading, uniform loading, and triangular loading. They concluded that the behavior and shear strength of cantilevers

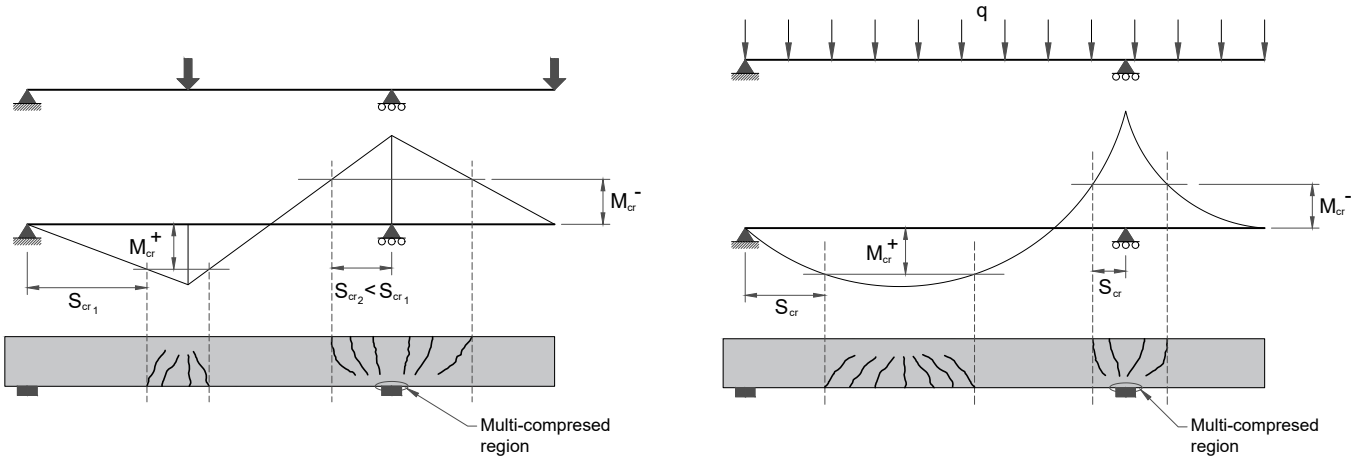

Figure 10. Location of critical section in cantilevers and in simply supported regions.

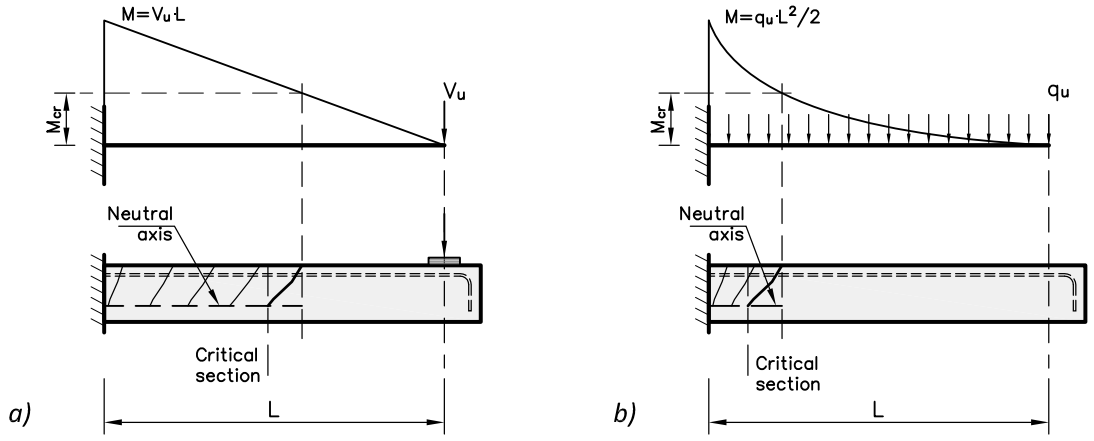

Figure 11. Location of critical section in a cantilever, under concentrated and distributed loading.

are very different from that of simply supported beams subjected to distributed loading, and the type of loading significantly affects the shear strength. For the constant-depth cantilevers tested, the same elements carried 27% more load for uniformly distributed loading than for point loading, and more than 100% for triangular loading than for point loading.

According to the CCCM, the critical shear crack starts from a flexural crack, at a section where the bending moment at shear failure is equal to the cracking moment of the cross section. Then, in the case of cantilevers, the distance from the initiation of the critical shear crack to the support is much lower than in the sagging region, as shown in Figure 10. Therefore, a multi-compression state of stresses is generated around the support and an enhancement of shear strength similar that taking place in continuous beams, occurs.

Similarly, in cantilevers subjected to distributed loading, the critical shear crack starts closer to the support than in the case of a concentrated load (see figure 11), resulting in the same effect.

5.5. Why the position of critical shear crack depends on the amount of longitudinal and transverse reinforcements? Which is the importance of such position?

As already mentioned, the higher is the reinforcement ratio, the higher are the shear and flexural strengths. Thus, as the cracking moment is almost independent of the amount of longitudinal reinforcement, the point where the bending moment law at shear failure equals the cracking moment $x_{cr}=M(x)/V_u=M_{cr}/V_u$ (where the critical crack starts, according to CCCM), will be closer to the support as the higher is the longitudinal reinforcement because the shear strength is higher.

Furthermore, beams with shear reinforcement have a higher shear capacity than beams without shear reinforcement. Following the same reasoning as before, the critical shear crack in beams with shear reinforcement will be closer to the support than for the same type of beams without shear reinforcement.

The position of the critical crack may be determinant in cases where the anchorage of the longitudinal reinforcement is exclusively provided by bond, as it is the case of prestressed pre-tensioned concrete beams. This is especially relevant in the case that bond strength between the strand and the concrete is low or is reduced by corrosion. In addition, the position of the critical crack indicates the position where, according to CCCM, should be verified the shear strength (control section), placed at a distance 0.85d of the crack initiation in the direction of increasing bending moments. Therefore, it results that in the case of prestressed concrete members, the satisfaction of the shear strength in cracked zones must be done at a higher distance from the support than in the case of reinforced concrete beams.

5.6. Do a rectangular RC beam and a T beam with the same effective depth and web width resist the same shear?

According to the linear elastic methods, historically used in structural design, bending is resisted by the tension and compression chords, while shear is taken by the web. However, experimental studies [44–50] have shown that a significant increment in the shear strength of slender RC beams with T-shaped section takes place with respect to beams with equal height, web width and reinforcements amounts, see Figure 12, [44].

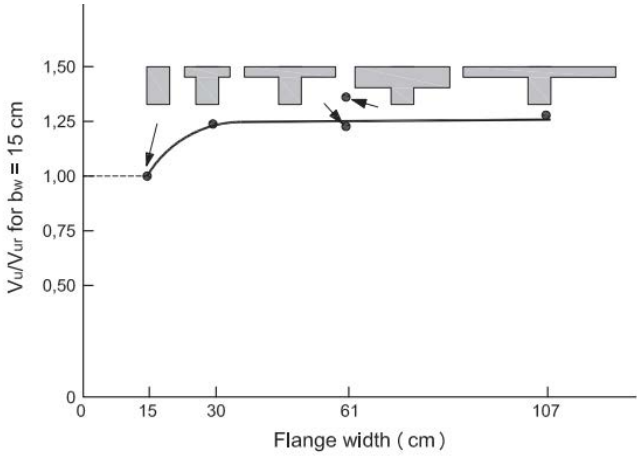

Figure 12. Effects of flanges on shear strength in beams with T-shaped cross section.

In addition, rigorous theoretical and numerical studies [51–52] have confirmed such concentration of shear stresses towards the neighborhood of the crack tip and towards the concrete compression chord, which in T beams is usually located in the flanges. Such stresses extend inside the flanges diminishing its intensity with the distance to the web (see Figure 13),[51].

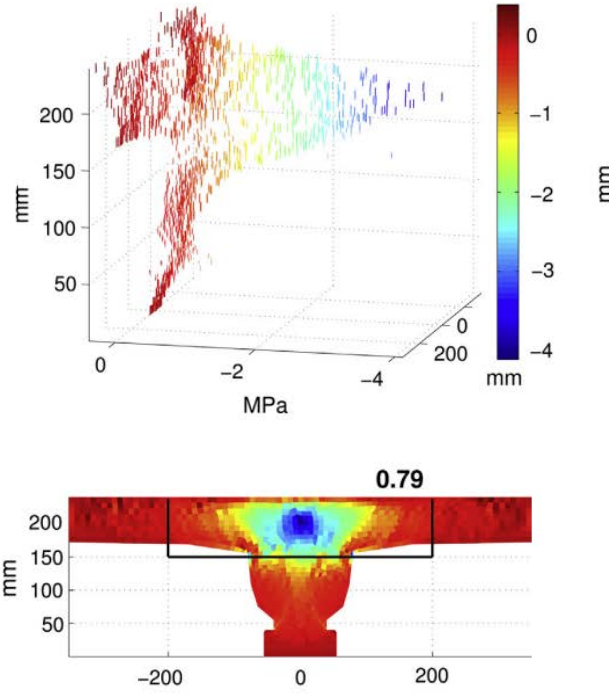

Figure 13. Concentration of shear stresses in the compression chord extending to the flanges [51].

To account for this phenomena in a simplified way, a "Shear effective flanges width" was defined as a flange width that, assuming a constant shear stresses distribution in the transverse direction, would provide the same shear force in the flanges than the actual shear stresses distribution (Figure 14).

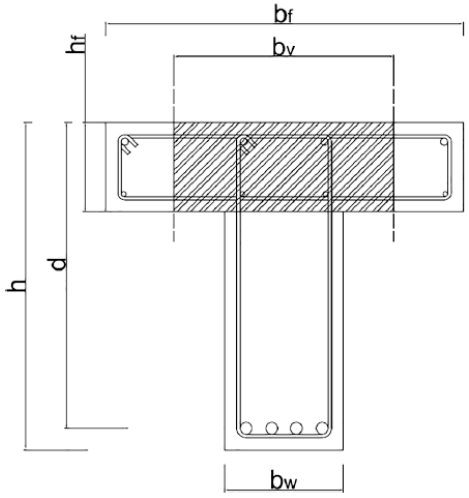

Figure 14. The "shear effective flanges width" in T shaped beams, adopted by the CCCM [49].

Such concept, previously developed [47], was incorporated into MASM and CCCM models by Cladera *et al.* [53]. The proposed value of the flanges effective shear width was obtained by considering that the flow of shear stresses $f(z)=\tau(z)\cdot b(z)$ has a parabolic profile (section 4), and that the widths of the zones where the shear stresses are integrated depend on the position of the neutral axis with respect to the depth of the flanges, as indicated by Eq. 14a and 14b below:

$$if\ x \le h_f \rightarrow b_{v,eff} = b_w + 2h_f \le b \tag{14a}$$

$$if\ x \le h_f \rightarrow b_{v,eff} \approx b_w + (b_v - b_w)\left(\frac{h_f}{x}\right)^{3/2} \tag{14b}$$

Other beneficial effects of the T or I sections is the confinement of the concrete in the core between the flanges and the web, provided both by the concrete flanges and by the transverse reinforcement, if present. Such enhancement can be taken into account by the MASM and the CCCM through the normal transverse stress σ_z , as it occurs with the stresses produced by moments tangential to the perimeter of a column in the case of punching shear of flat slabs [40].

Since an accurate assessment of existing bridges and other transportation infrastructures, which are often being built with T-shaped cross section members, requires a realistic evaluation of the structure strength, models that account for the flanges contribution provide a more realistic approach and can be very useful in the assessment of existing structures.

5.7. Does an axial compression force influence the shear strength to the same extent as a tensile force?. How does prestressing eccentricity influence the shear strength?

Moderate compressive axial stress increases the depth of the compression block for equilibrium reasons, delays cracking due to the reduction of the principal tensile stresses, and reduces

crack width, and the inclination of the concrete struts (higher cotθ). Consequently, the contributions V_c, V_w and V_s increase. This effect is accounted for in the MASM and CCCM models through x/d, which in turn influences the angle of the cracks, since cotθ=0.85/(1-x/d). Therefore, the higher the compression axial force, the larger x/d and larger cotθ. According to Mari *et al* [54], the neutral axis depth in members subjected to an external axial compression "N_E" may be obtained by:

$$N_E \geq 0 \rightarrow x = x_0 + 0.80(h - x_0)\left(\frac{d}{h}\right)\frac{\sigma_{cp}}{\sigma_{cp}+f_{ctm}} \leq h \qquad (15)$$

where x_0 is the neutral axis depth of the element assuming N=0 and σ_{cp}=N/A is the mean compression stress. It is important to note that the ratio σ_{cp}/f_{ct} is decisive in the calculation of x/d and, therefore, in the shear strength of prestressed concrete members.

In addition, the eccentricity of prestressing increases the shear strength, because the prestressing moment P·e, is contrary to the moment generated by external loads and, additionally, increments the cracking moment. These effects are accounted for by the MASM and CCCM models, including the prestressing force P and its eccentricity into the equilibrium equations, in which the cracking moment of the prestressed section is included [54].

Under axial tensile stress, the depth of the compression block is reduced, the cracks are widened, and the angle of inclination of the struts is increased, thus decreasing cotθ. Consequently, the shear strength decreases, as concluded by D. Fernandez *et al.* [55], and Marí *et al.* [56] for beams and by P. Fernandez *et al*, [57] for punching in slabs subjected to in plane tension forces. According to MASM and CCCM models the depth of the neutral axis can be estimated as:

$$N_E < 0 \rightarrow x = x_0\left(1 + 0.1\frac{N_E\, d}{M_E}\right) \geq 0 \qquad (16)$$

In addition, under severe axial load, tensile flexural reinforcement may prematurely yield, causing a further reduction of the shear strength, Fernandez *et al.* [57]

5.8. How the compressive and tensile concrete strengths influence the shear strength of reinforced and prestressed concrete beams?

Some shear strength equations are expressed in terms of fcd, others in terms of $(f_{ck})^{1/3}$ and some in terms of $(f_{ck})^{1/2}$, what may generate confusion. As already mentioned, concrete is subjected to a multi-axial stress state, so its strength in one direction is affected by the stress in the orthogonal direction. For example, according to EC2, in the struts, a reduction factor 0.6 of the uniaxial compressive strength in the struts direction, is used to account for the orthogonal tensile stresses.

In the compression chord, concrete is subjected to a bi-axial compression-tension state of principal stresses and failure starts when at any point the biaxial failure envelope, is reached. The MASM and CCCM adopts the Kupfer and Gerstle failure envelope [35], see Figure 15, assuming the following linear equation for the tension-compression branch.

$$\frac{\sigma_1}{f_{ct}} + 0.8\frac{\sigma_2}{f_{cc}} = 1 \qquad (17)$$

Therefore, according to Eq. (17), both compression and tension concrete strengths influences the strength of the compression chord.

From Eq. (17), the principal tensile and compression stresses can be expressed as indicates Eq. (18), where the terms inside the parenthesis are the reduction factors due to the orthogonal stresses:

$$\sigma_1 = \left(1 - 0.8\frac{\sigma_2}{f_{cc}}\right) f_{cc}\ ; \quad \sigma_2 = 1.25\left(1 - \frac{\sigma_1}{f_{ct}}\right) f_{cc} \qquad (18)$$

Therefore, the MASM/CCCM fundamental equation (1) could be expressed indistinctly in terms of the tensile strength f_{ct} or in terms of the compressive strength f_{cc}, accounting for the respective reduction factor due to the orthogonal stresses.

5.9. Why mechanical shear models that consider different dominant shear transfer actions provide similar shear strength?

Figure 16, [54] shows the typical experimentally obtained load-displacement curve of a beam subjected to shear. In multiple tests, it has been observed that after the second branch of the critical crack develops, the load capacity generally does not significantly increase further, as softening of the concrete in the compression zone, which is subjected to both compressive and shear stresses, begins. This behavior has also been reported by other researchers in tests of notched specimens designed to study mixed-mode crack propagation through reinforced concrete, [59] shown in Figure 16. In fact, the last phase of crack propagation, when the crack changes its trajectory and gets

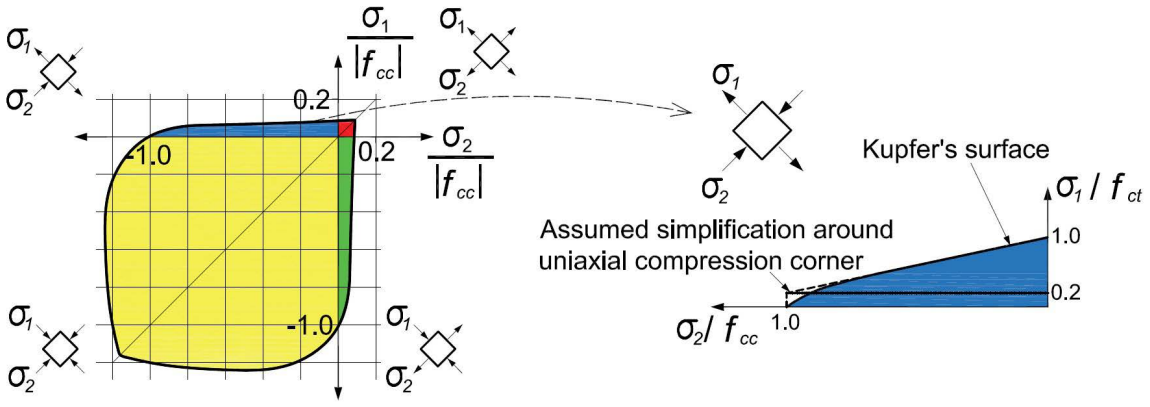

Figure 15. Kupfer and Gerstle biaxial failure envelope adopted.

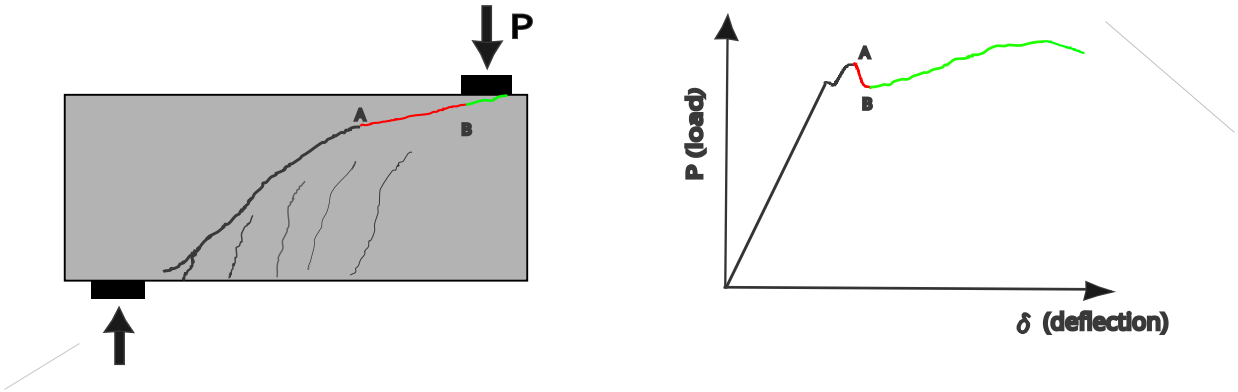

Figure 16. Load-displacement curve, crack propagation, and shear capacity models.

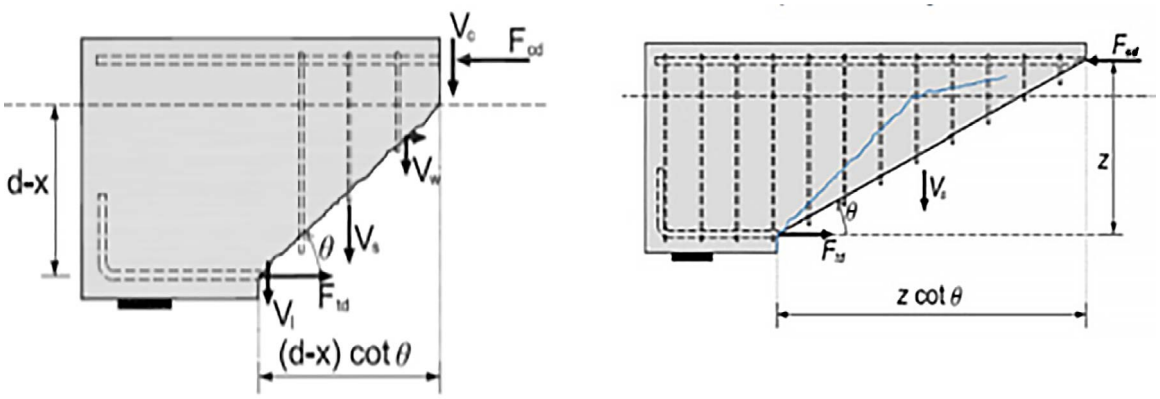

a) b)

Figure 17. Schematic critical crack and forces in a) MASM and CCM b) Shear friction models.

more inclined, is typically unstable, in the sense that it is due to an energy release rate that equals the energy needed for the propagation. This is clear in Figure 16 since almost no external energy is provided from point A to point B according to the load-deflection.

According to the load-deflection curve of Figure 16 right, a redistribution of internal forces may occur between load stages A and B and that while the shear resisted by the uncracked chord diminishes, the aggregate interlock in the compression chord increases (red branch, between A and B), until crushing of the compressed chord or loss of anchorage of the longitudinal reinforcement occurs. As the difference in values of the resisted load between points A and B is usually small, there are models that are proposed to capture the load at point A, while other models that try to capture the situation at failure (point B).

The models that try to obtain point A, incorporate the strength of the uncracked chord just before the crack propagates inside it. For this reason, the neutral axis depth and V_c are high. In turn, since the crack in the tension zone is very open, and the compressed zone above the tip prevents any meaningful contribution of shear slip along the crack interface, the contributions of aggregate interlock and dowel action are considered small compared to V_c (Figure 17a)

On the contrary, the models that seek to find point "B", consider the critical crack fully develops and the depth of the compressed block at the end of the crack is very small, resulting in a very low value of V_c. However, they incorporate the friction force along the second branch of the critical shear crack as a part of the aggregate interlock, whose vertical component is considered to be incorporated as V_w, Figure 17b. This has been observed in numerous tests, thanks to today's capacity to measure displacements using Digital Image Correlation, Cavagnis [60], and Montoya-Coronado *et al.* [61]. The next step is to show, through theoretical approaches, that the sum of the shear transfer actions in points A and B are very close.

MASM and CCCM models are among those based on the contribution of the compression chord as dominant shear transfer action, so the shear strength predicted corresponds to point A in Figure 16. Thus, it is relevant to show the accuracy and robustness of these methods when predicting the shear strength in multiple situations.

In fact, the MASM, and subsequently the CCCM, were originally developed for reinforced concrete slender members with and without shear reinforcement made of steel, and rectangular cross section [3-4]. Subsequently it was extended to reinforced concrete beams with T and I sections [53], prestressed concrete members [54], members subjected to tension axial loads [56], beams reinforced with FRP longitudinal [62] and shear reinforcements [63], to steel fiber reinforced concrete beams (SFRC) [64], to non-slender beams [36], to punching of slabs under symmetrical loading [40] and to punching of slabs subjected also to in-plane axial tensile forces

TABLA 2.
Verification of the proposed model: mean value, COV and 5% percentile for V_{test}/V_{pred} ratio.

Type of member tested	No. Tests	Mean	CoV	Percentile 5%
RC slender beams, rect. section w/o shear reinf.	784	1.170	0.185	0.800
RC slender beams, rect. section with shear reinf.	170	1.160	0.141	0.800
RC slender Beams , T/I section w/o shear reinf.	188	1.020	0.192	0.790
RC slender Beams , T/I section with shear reinf.	70	1.140	0.149	0.870
PC slender beams, w/o shear reinforcement	214	1.180	0.165	0.818
PC slender beams, with shear reinforcement	117	1.170	0.186	0.775
FRP reinforced concrete beams w/o shear reinf.	144	1.090	0.148	0.830
FRP reinforced concrete beams with shear reinf.	112	1.080	0.195	0.750
RC non-slender beams without web reinf.	153	1.350	0.267	0.752
RC non-slender beams with vertical web reinf.	171	1.250	0.193	0.898
RC-non slender beams with vert. and horiz. web reinf.	86	1.280	0.223	0.935
SFRC slender and non-slender beams w/o shear reinf.	488	1.150	0.220	0.780
Symmetric punching in slabs w/o shear reinf.	328	1.188	0.151	0.905
Symmetric punching in slabs with shear reinf.	232	1.173	0.149	0.774
Punching and tensile force in slabs w/o shear reinf.	38	1.11	0.093	0.975

[57]. Further extension of these models is currently being carried out, i.e. to punching of eccentrically loaded slabs, to slabs strengthened with post-installed studs and to SFRC slabs, to prestressed concrete beams using FRP tendons including the loss of bond strength in pre-tensioned beams, to composite members made of reinforced or prestressed concrete beams and cast-in-place slabs.

A comparison between the shear strength predicted by the CCCM ($V_{u,theo}$) and the experimental shear strength ($V_{u,exp}$), measured in 3295 tested members, included in 16 different previously published shear-databases, has been made, updating the work previously done by Cladera *et al* [65].

The statistical results show that the theoretical predictions are reasonably safe, precise and with low scatter. The mean value of the ratio $V_{u,exp}/V_{u,pred}$, ranges between 1.02 and 1.35, the minimum value of the 5% percentile is 0.75, indicating that the 95% of the data have a ratio $V_{u,exp}/V_{u,pred}$ greater than 0.75. Finally, the CoV ranges between 0.093 and 0.267, which is considerably low, despite the complexity of the shear behavior, the uncertainties associated to the tensile concrete strength and the variety of cases studied, among many other factors.

6. CONCLUSIONS

- In this paper, some questions on shear behavior and strength, that arise from a limited understanding of the shear resisting mechanisms when using empirical models are raised. Answers to these questions have been provided according to mechanical shear models, based on the contribution of the uncracked concrete zone as main shear transfer action.
- The following aspects have been addressed and clarified:
  - The influence of the longitudinal reinforcement, the shear slenderness, the axial tension or compression forces and the local stresses near applied concentrated loads or reactions on the shear strength.
  - The reasons for the differences existing between the shear strength of simply supported, continuous beams and cantilevers
  - The contribution of the flanges in T or I shaped beams to the shear strength
  - How the location of the critical crack can be determined based on the hypothesis of the CCCM, and its relevance to identify the position of the control section and to quantify the strength of a bond anchorage.
- A rational explanation to why models that consider different dominant shear transfer actions drive to quite similar results, has been provided, based on the redistributions between shear transfer actions, along the incremental loading process. A way to develop a unified theory, which would ease performance-based shear design remains open.
- The answers provided to the questions raised, show the capacity of the mechanical models, and in particular the MASM and CCCM, to provide an insight into the shear behavior. This fact, together with the simplicity of the proposed equations and the accuracy obtained in the comparisons with 3295 experimental results, including a large variety of situations, prove these models to be adequate for carrying out performance-based shear design, as well as for assessment and strengthening of existing structures

Acknowledgements

This article collects some of the results obtained and lessons learned during the development of the MASM and CCCM in the framework of the coordinated research project BIA2015-64672-C4-1-R, financed by the Ministry of Science and Innovation of Spain, and ERDF Funds. The author wishes to express his gratitude to the direct participants in this collective work, Drs. Jesús M. Bairán, Eva Oller, Noemí Duarte, Raúl Menduiña, Tomás García, from UPC and to Antoni Cladera, Carlos Ribas, Joaquín Pinilla and Luis Montoya from UIB. Likewise, I would like to also thank Profs. Fernando Martínez,

Manuel Herrador and Fernando Varela Puga, from UdC, Pedro Miguel, Jose L Bonet and Miguel A. Fernández from UPV, for their contributions as members of the coordinated project. Finally, special thanks are given to Profs. Juan Carlos Arroyo (Univ. Nebrija/CALTER), Juan Navarro Gregori (UPV), Gonzalo Ruiz (UCLM), David Fernández (UPM), and Juan Murcia-Delso (UPC), for their wise suggestions and constructive criticism, so useful to continue advancing.

References

[1] Ritter, W. (1899). Die Bauweise Hennebique. Shweizerische Bauzeitung, 33(7), 59-61

[2] Morsch E. Concrete-Steel Construction (Der Eisenbetonbau), English translation of the 3rd German edition. New York: McGraw-Hill Book Co.; 1909.

[3] A. Marí, J.M. Bairan, A. Cladera, E. Oller, C. Ribas, Shear-flexural strength mechanical model for the design and assessment of reinforced concrete beams, Structure and Infrastructure. Engineering 11 (2015) 1399–1419.

[4] A. Mari, A. Cladera, JM. Bairan, J., E. Oller, E., C. Ribas, Un modelo unificado de resistencia a flexión y cortante de vigas esbeltas de hormigón armado bajo caras puntuales y repartidas. Hormigón y Acero 65 (2014) no.274 247-265.

[5] A. A. Cladera Marí, J.M. Bairán, C. Ribas, E. Oller, N. Duarte, The compression chord capacity model for the shear design and assessment of reinforced and prestressed concrete beams, Structural Concrete 17 (2016) 1017–1032.

[6] ACI-ASCE Committee 445, Recent approaches to shear design of structural concrete, J. Struct. Eng. 124 (1998), no 12 1375–1417.

[7] J.M. Bairán, A. Marí, Coupled model for the nonlinear analysis of anisotropic sections subjected to general 3D loading. Part 2: Implementation and validation, Computer and Structures 84 (2006) nos 31-32 2254-2276.

[8] F. Cavagnis, M. Fernández, A. Muttoni, An analysis of the shear-transfer actions in reinforced concrete members without transverse reinforcement based on refined experimental measurements, Structural Concrete 19 (2018) 49-64.

[9] J. Bairán, A. Marí, A. Cladera, Analysis of shear resisting actions by means of optimization of strut and tie models taking into account crack pattern, Hormigón y Acero. 69 (2017) no. 286 197-206.

[10] D. Fernandez, Mecanismos de respuesta frente al esfuerzo cortante en vigas prefabricadas, Doctoral Thesis. Supervisor A. Aparicio, Polytechnic University of Madrid . (2001).

[11] F. J. Vecchio, M.P. Collins, The Modified Compression Field Theory for Reinforced Concrete Elements Subjected to Shear, ACI Journal Proceedings, 83 (1986) no. 2 219-231.

[12] CSA Committee A23.3, Design of Concrete Structures, CSA Group, Toronto, Canada (2004).

[13] AASHTO, LRFD Bridge Design Specifications, eighth edition, American Association of State Highway and Transportation Officials, Washington, DC, (2017).

[14] E. C. Bentz, M. P. Collins, Updating the ACI Shear Design Provisions, Concrete International 39, (2017), No. 9 33-38.

[15] A. Muttoni, M. F. Ruiz, Shear strength of members without transverse reinforcement as function of critical shear crack width, ACI Structural Journal 105 (2008) 163–172.

[16] M. F. Ruiz, A. Muttoni, J. Sagaseta, Shear strength of concrete members without transverse reinforcement: A mechanical approach to consistently account for size and strain effects, Eng. Structures, 99 (2015) 360–372.

[17] Fib Model Code 2010, Final Draft, Volume 1 fib Bulletins N° 65. Lausanne, Switzerland, 2012.

[18] Y. Yang, J. Walraven, Den Uijl, J. Shear Behavior of Reinforced Concrete Beams without Transverse Reinforcement Based on Critical Shear Displacement. Journal of Structural Engineering, 143 (2017) no. 1. [04016146]. https://doi.org/10.1061/(ASCE)ST.1943-541X.0001608.

[19] J.C. Walraven. Fundamental analysis of aggregate interlock, Journal of the Structural Division, Proceedings of the ASCE, 107 (1981), no 11 2245-2270.

[20] M.P. Nielsen, Limit analysis and concrete plasticity, London: Prentice-Hall, (1984).

[21] J. Schlaich, K., Schafer, M. Jennewein, Toward a consistent design of structural concrete, PCI Journal, 32 (1987). No. 3. 74-150.

[22] CEN. EN 1992, Eurocode 2: Design of concrete structures- Part 1-1: General rules and rules for buildings, Brussels: Comité Européen de Normalisation, (2005).

[23] K.H. Reineck, Ultimate shear force of structural concrete members without transverse reinforcement derived from a mechanical model, ACI Structural Journal 88 (1991) no.5 592-602.

[24] ZP. Bazant, JK. Kim, Size effect in shear failure of longitudinally reinforced beams, ACI Structural Journal, 85 (1984) no. 5 456-468.

[25] ACI Committee 318, Building Code Requirements for Structural Concrete (ACI 318-19), American Concrete Institute (2019).

[26] Daniel A. Kuchma, Sihang Wei, David H. Sanders, Abdeldjelil Belarbi, and Lawrence C. Novak, Development of the One-Way Shear Design Provisions of ACI 318-19 for Reinforced Concrete. ACI Structural Journal 116 (2019) no. 4 285-295.

[27] A. Hillerborg, Analysis of a single crack. Fracture Mechanics on Concrete, Development in Civil Engineering. Elsevier Science Publishers, Amsterdam (1983).

[28] JR. Carmona, G. Ruiz, Bond and size effects on the shear capacity of RC beams without stirrups", Engineering Structures 66 (2014) 45-56.

[29] MD. Kostovos, J. Bobrowsky, J. Eibl, Behavior of reinforced concrete T-beams in shear, Structural Engineer, Part B: R&D Quarterly, 65 (1987), B1 1-10.

[30] PD. Zararis, G.CH. Papadakis , Diagonal shear failure and size effect in RC beams without web reinforcement, Journal of Structural Engineering 127 (2001) no.7 733-741.

[31] AK. Tureyen, RJ. Frosch, Concrete Shear Strength: Another Perspective," ACI Structural Journal, V. 100 (2003) no. 5 609-615.

[32] HG. Park, KK. Choi, JK, Wight. Strain-based shear strength model for slender beams without web reinforcement, ACI Structural Journal 103 (2006) no. 6 783–793.

[33] YA Li, TC Hsu, SJ Hwang, Shear Strength of Prestressed and Non-prestressed Concrete Beams, Concrete International, 39 (2017) no. 9 53-57.

[34] A. Cladera, JL Pérez-Ordóñez, F. Martínez-Abella, Shear strength of RC beams. Precision, accuracy, safety and simplicity using genetic programming. Comput Concr. 14 (2014) 479–501.

[35] HB Kupfer, KH. Gerstle, Behavior of concrete under biaxial stresses, J Eng Mech Div 99 (1973) 853–866.

[36] J.M. Bairán, R. Menduiña, R., A. Marí, A. Cladera, Shear Strength of Non-Slender Reinforced Concrete Beams, ACI Structural Journal, 117 (2020) no. 2 277-279. https://doi.org/10.14359/51721369.

[37] R. Vaz Rodrigues, A. Muttoni, and M. Fernández Ruiz, Influence of shear on rotation capacity of reinforced concrete members without shear reinforcement, ACI Struct. J. 107 (2010) no. 5 516–525.

[38] A. Montserrat, P. Miguel, JL. Bonet, MA. Fernandez, Influence of the plastic hinge rotations on shear strength in continuous reinforced concrete beams with shear reinforcement, Engineering Structures 207, (2020) 110242. https://doi.org/10.1016/j.engstruct.2020.

[39] A. Montserrat, P. Miguel, JL. Bonet, MA. Fernandez, Experimental study of shear strength in continuous reinforced concrete beams with and without shear reinforcement, Engineering Structures 220 (2020) 110967. https://doi.org/10.1016/j.engstruct.2020.

[40] A. Marí, A. Cladera, E. Oller, JM. Bairán. A punching shear mechanical model for reinforced concrete flat slabs with and without shear reinforcement, Engineering Structures 166 (2018) 413-426.

[41] N. Bagge N., A. O'Connor, L. Elfgren, C. Pedersen, Moment redistribution in RC beams – A study of the influence of longitudinal and transverse reinforcement ratios and concrete strength. Engineering Structures 80 (2014) 11-23.

[42] DIANA User's Manual. Release 10.5. (2021). DIANA FEA. BV.

[43] A. Perez, P. Padilla, A. Muttoni, M. Fernández, Effect of Load Distribution and Variable Depth on Shear Resistance of Slender Beams without Stirrups, ACI Struct. J. 5 (2012) no 5 595-604.

[44] Leonhardt, F. Walther R, The Stuttgart Shear Tests, (1961). C&CA Translation, No. 111, Cement and Concrete Association, 1964, London.

[45] PM. Ferguson, JN. Thompson, Diagonal Tension in T-Beams Without Stirrups, ACI J Proc. 49 (1953) 665–675.

[46] MW. Kani, MW. Huggins MW, RR.Wittkopp, Kani on shear in reinforced concrete, Dept. of Civil Engineering, University of Toronto (1979).

[47] Placas A, Regan PE, Shear failure of reinforced concrete beams. J American Concrete Institute 68 (1971) no. 7 63–73.

[48] C. Giaccio R. Al-Mahaidi R, G.Taplin, Experimental study on the effect of flange geometry on the shear strength of reinforced concrete T-beams subjected to concentrated loads. Can J Civ Eng. 29 (2011) no. 6 911–918. https://doi.org/10.1139/l02-099.

[49] C. Ribas, A. Cladera, Experimental study on shear strength of beam-and-block floors. Eng Struct. 57 (2013) 428–42. https://doi.org/10.1016/j.engstruct.2013.10.001.

[50] ACI-ASCE Committee 426, The Shear Strength of Reinforced Concrete Members, ACI J. Proc. 70 (1973) 1091–187.

[51] C. Ribas Gonzalez. Resistencia a cortante de los forjados de vigueta pretensada y bovedilla. Doctoral Thesis. Universitat Politècnica de Catalunya. Department of Construction Engineering (2013).

[52] A. Ayensa, E. Oller, B. Beltrán, A. Marí, L. Gracia, Influence of the flanges width and thickness on the shear strength of reinforced concrete beams with T-shaped cross section, Engineering Structures 188, (2019) 506-518.

[53] A. Cladera , A. Marí, J.M Bairán, C. Ribas, Predicting the shear–flexural strength of slender reinforced concrete T and I shaped beams, Eng. Struct. 101 (2015) 386–398.

[54] A. Marí, J.M. Bairán A. Cladera and E. Oller, Shear design and assessment of reinforced and prestressed concrete members based on a mechanical model, ASCE Journal of Structural Engineering 142 (2016) no.10 1-17.

[55] D. Fernández, E. Gonzalez, E. Diaz, Influence of axial tension on the shear strength of floor joists without transverse reinforcement, Structural Concrete 16 (2015) no. 2 207-220.

[56] A. Marí, J. M. Bairán, A. Cladera, Effects of axial forces and prestressing on the shear strength of structural concrete members, Hormigón y Acero, 68 (2017). Proceedings International Congress of Structures, ACHE, A Coruna, June 2017.

[57] P.G. Fernández, A. Marí, E. Oller, Theoretical prediction of the punching shear strength of concrete flat slabs under in-plane tensile forces, Engineering Structures 229 (2021) 111632.

[58] A. Cladera, A. Marí, J.M. Bairán, E. Oller, C. Ribas, One-Way Shear Design Method Based on a Multi-Action Model, Concrete International, 39 (2017) no. 9 1-8.

[59] J.R. Carmona, G. Ruiz, and J.R. del Viso, Mixed-Mode Crack Propagation through Reinforced Concrete, Engineering Fracture Mechanics 74 (2007) no.17 2788-2809.

[60] F. Cavagnis, M. Fernandez, A. Muttoni, An analysis of the shear-transfer actions in reinforced concrete members without transverse reinforcement based on refined experimental measurements, Structural Concrete 19 (2017) no.10 https://doi.org/10.1002/suco.201700145.

[61] L. Montoya-Coronado, C. Ribas, J. Ruiz-Pinilla, A. Cladera, Time-History Analysis of Aggregate Interlock in Reinforced Concrete Beams without Stirrups, Engineering Structures 283 (2023) 115912, https://doi.org/10.1016/j.engstruct.2023.115912

[62] A. Marí; A. Cladera; Oller, E.; J.M. Bairán, Shear design of FRP reinforced concrete beams without transverse reinforcement, Composites Part B: Engineering 57 (2014). 228-241 https://doi.org/10.1016/j.compositesb.2013.10.005.

[63] E. Oller, A. Marí, J.M. Bairán, A. Cladera, Shear design of reinforced concrete beams with FRP longitudinal and transverse reinforcement, Composites Part B: Engineering 74 (2015) 104 - 122.

[64] A. Marí, N. Spinella, A. Recupero, A. Cladera, Mechanical model for the shear strength of steel fiber reinforced concrete (SFRC) beams without stirrups, Materials and Structures 53 (2020) no. 28 https://doi.org/10.1617/s11527-020-01461-4.

[65] A. Cladera, A. Marí, C. Ribas, E. Oller, J. M. Bairán, N. Duarte, R. Menduiña, A simplified model for the shear strength in RC and PC beams, and for punching shear in slabs, without or with shear reinforcement, including steel, FRP and SMA. SMAR 2019- 5th conference on Smart monitoring, assessment and rehabilitation of structures.

APPENDIX 1.

SHEAR DESIGN OF A REINFORCED CONCRETE SHORING BEAM BY MEANS OF THE CCCM

A1.1 Definition of the structure

Consider a continuous reinforced concrete shoring beam of two equal spans of 6 m, that must resist two concentrated variable loads of Q_d=300 kN each, fixed at midspan. The self-weight is ignored for the sake of simplicity. The cross section is rectangular of dimensions b=400m, h=550mm, and an effective depth d=500 mm is assumed. Figure A1.1 shows the structural scheme and the design bending moments and shear forces laws. The longitudinal reinforcement in the bottom consists of a basic reinforcement of 3ϕ20 along the whole beam and an additional reinforcement of 2ϕ20+2ϕ16 placed in a length of 4.5m from the end supports. At the top, the basic reinforcement consists of 4ϕ16 bars and the additional reinforcement consists of 3ϕ20 extended to 3 m length at both sides of the intermediate support axis, as shown in Figure A1.2

Concrete characteristic strength is 25 MPa (γ_c = 1.50), Yield strength of both longitudinal and transverse reinforcements is 500 MPa (γ_s = 1.15), but the design strength of the transverse reinforcement is limited to f_{ywd}=400 MPa, for cracking control reasons.

A1.2. Design of the reinforcement near the end supports

According to the CCCM, the section where the shear reinforcement should be designed is where at shear failure the bending moment equals the cracking moment, M(scr)=Mcr. For a point load, the bending moment is linear, M(x)=Vd·x, so being the cracking moment of the beam Mcr=51.6 kNm, and Vd = 121.8 kN the design shear force corresponding to the end supports zones, the position of the section where the critical crack starts is scr=Mcr/Vd=51.6/121.8=0.42m. For design purposes, since the shear force is constant Vd=121.8 kN, no matter the section considered. In the case that the shear force law is not constant, the section where the critical crack starts should be obtained equaling the bending moment to the cracking moment. Assuming a uniformly distributed load "g", where the design shear force is Vd=Rd= αgL the design section would be:

$$s_{cr} = \alpha L \left(1 - \sqrt{1 - \frac{M_{cr}}{M_{max}}}\right) \qquad \text{(A1.1)}$$

For two equal spans, α=0.375 and M_{max}=0.0703 ql^2.

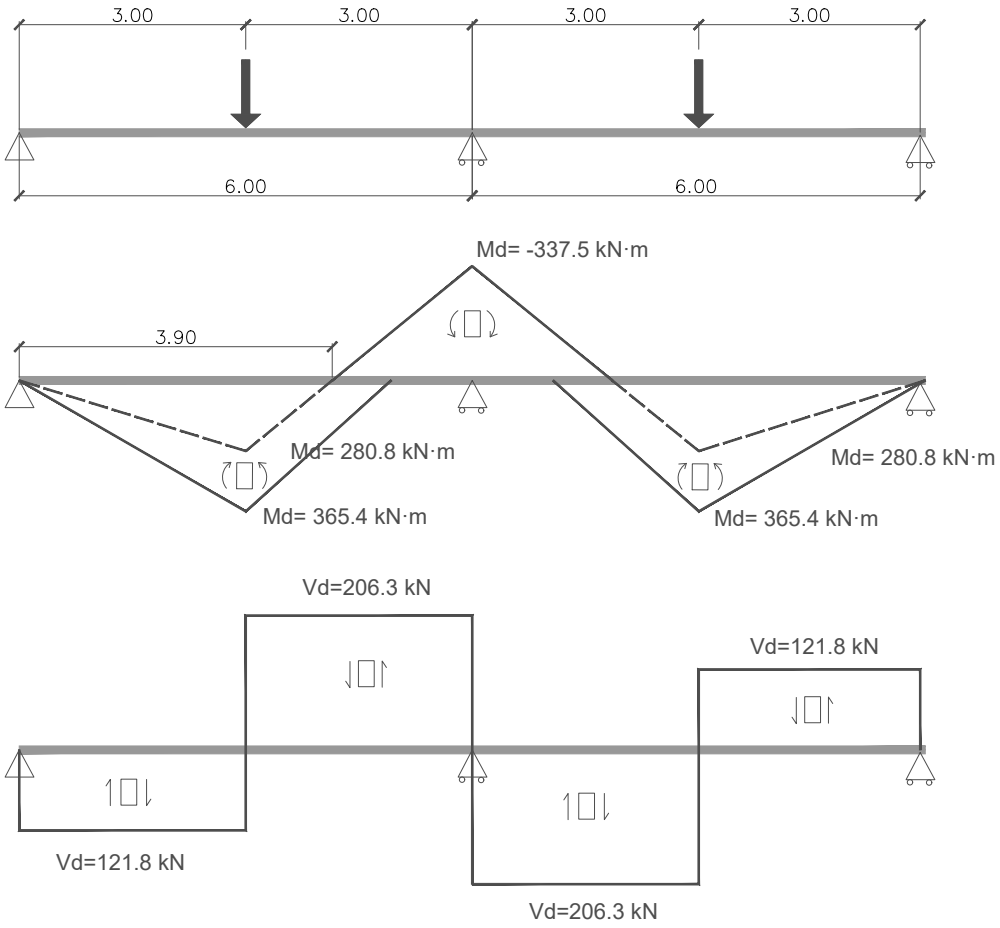

Figure A1.1. Structure scheme and design bending moments and shear forces laws.

Longitudinal reinforcement area: 5 ϕ20 + 2ϕ16 = 1972 mm²

Concrete properties and neutral axis depth:

$$F_{cd} = \frac{f_{ck}}{\gamma_c}\ 16.67\ MPa\ ;\ f_{ctm} = 0.30\sqrt[3]{f_{ck}^2} = 2.56\ MPa$$

$$E_{cm} = 22000\left(\frac{f_{cm}}{10}\right)^{0.3} = 22000\left(\frac{33}{10}\right)^{0.3} = 31475\ MPa;$$

$$\alpha_E = \frac{E_s}{E_{cm}} = 6.35$$

$$\rho_l = \frac{A_s}{bd} = \frac{1972}{400{\cdot}500} = 0.000986;$$

$$\frac{x}{d} = n\rho_l\left(-1+\sqrt{1-\frac{2}{n\rho_l}}\right) = 0.296; \qquad x = 148\ mm$$

The shear span to effective depth ratio, a/d, at each region, should be calculated for the load combination that produces maximum shear, and its concomitant bending moment. For the case of the shear near the end supports, such combinations correspond to a single point load applied, for which V_d=121.8 kN and M_d=365.4 kNm.

Which is less than the minimum shear reinforcement

Size effect: $\frac{a}{d} = \frac{M_d}{V_d\, d} = \frac{365}{121.8{\cdot}0.5} = 5.99$

$$\zeta = \frac{2}{(5.99)^{0.2}\sqrt{1+\frac{500}{200}}} = 0.747$$

$$V_{cu} = 0.3\,\zeta\frac{x}{d}f_{cd}^{2/3}b_{v,eff}\,d = 0.3{\cdot}0.747{\cdot}0.296{\cdot}16.67^{2/3}{\cdot}400{\cdot}500 = 86.5KN \not< V_{cu,min}$$

$$V_{cu,min} = 0.25\left(\zeta K_c + \frac{20}{d_0}\right)f_{cd}^{2/3}b_w\,d = 0.25\left(0.709{\cdot}0.20 + \frac{20}{500}\right)16.67^{2/3}400{\cdot}500 =$$

$$= 59.2\ kN$$

$$cot\theta = \frac{0.85d}{d-x} = \frac{0.85\cdot 500}{500-148} = 1.20 \le 2.50\ ;\quad \theta = 39.7^{\circ}$$

Design of the shear reinforcement

$$f_{ywd} = \frac{500}{1.15} = 435\ ;\ sin\alpha = 1\ ;\ cot\alpha = 0$$

$$V_{su} = V_d - V_{cu} = 121.8 - 86.5 = 35.3\ kN$$

$$V_{su} = 1.4\,\frac{A_{sw}}{s_t}f_{ywd}(d-x)\,sin\alpha\,(cot\theta + cot\alpha) = 238000\,\frac{A_{sw}}{s_t} = 35300\ N$$

$$\frac{A_{sw}}{s_t} = \frac{35300}{238000} = 0.148\,\frac{mm^2}{mm^2}$$

area per unit length:

$$\frac{A_{sw,min}}{s_t} = 0.08\, b_w \frac{\sqrt{f_{ck}}}{f_{yk}} = 0.03 \cdot 400\, \frac{\sqrt{25}}{500} =$$

$$= 0.35\ mm^2 / mm\ (\phi 8\ mm\ ,\ s=300\ mm)$$

Verification of the struts strength $V_{Ed} < V_{Rd,max}$

$$V_{Rd,max} = \alpha_{cw}\, b_w\, z v_1 f_{cd}\, \frac{cot\theta + cot\alpha}{1 + cot^2\theta} = 1 \cdot 400 \cdot 500 \cdot 0.9 \cdot 16.67\ \frac{1.20}{1 + 1.20^2}$$

$$= 885.3\ kN > V_{Ed} = 121.8\ kN$$

Then, minimum reinforcement, consisting of closed stirrups of ϕ8 mm, spaced 300 mm is placed.

A1.3. Design of the shear reinforcement near the intermediate support

Longitudinal reinforcement area: 3 ϕ20 + 4ϕ16 = 1746 mm²

$$\rho_l = \frac{A_s}{bd} = \frac{1746}{400 \cdot 500} = 0.0008732;$$

$$\frac{x}{d} = n\rho_l \left(1 + \sqrt{1 + \frac{2}{n\rho_l}}\right) = 0.282; \qquad x = 141\ mm$$

In this case, the maximum shear force near the central supports takes place under two loads applied, so M_d=-337.5 kNm and V_d=206.3 kN.

Size effect: $\frac{a}{d} = \frac{M_d}{V_d\, d} = \frac{337.5}{206.3 \cdot 0.5} = 3.27$

$$\zeta = \frac{2}{(3.27)^{0.2} \sqrt{1 + \frac{500}{200}}} = 0.843$$

$$V_{cu} = 0.3\, \zeta \frac{x}{d} f_{cd}^{2/3} b_{v,eff}\, d = 0.3 \cdot 0.843 \cdot 0.282 \cdot 16.67^{2/3} \cdot 400 \cdot 500 = 92.9 KN < V_{cu,min}$$

$$V_{cu,min} = 0.25 \left(\zeta K_c + \frac{20}{d_0}\right) f_{cd}^{2/3} b_w d = 0.25 \left(0.843 \cdot 0.20 + \frac{20}{500}\right) 16.67^{2/3} 400 \cdot 500 =$$

$$= 67.9\ kN$$

$$cot\theta = \frac{0.85d}{d - x} = \frac{0.85 \cdot 500}{500 - 141} = 1.18 \le 2.50\ ; \quad \theta = 40.2^\circ$$

Then, closed stirrups of ϕ8 spaced 200 mm are placed.

Design of the shear reinforcement

f_{ywd} = 400 MPa ; $sin\alpha = 1$; $cot\alpha = 0$

$V_{su} = V_d - V_{cu} = 206.3 - 92.9 = 113.4\ kN$

$$V_{su} = 1.4 \frac{A_{sw}}{s} f_{ywd} (d_s - x) sin\alpha (cot\theta + cot\alpha) = 240000 \frac{A_{sw}}{s} = 113400\ N$$

$$\frac{A_{sw}}{s_t} = \frac{113400}{240000} = 0.472\ \frac{mm^2}{mm^2}$$

$$V_{Rd,max} = \alpha_{cw}\, b_w\, z v_1 f_{cd}\, \frac{cot\theta + cot\alpha}{1 + cot^2\theta} = 1 \cdot 400 \cdot 500 \cdot 0.9 \cdot 0.6 \cdot 16.67 \frac{1.18}{1 + 1.18^2}$$

$$= 887.5\ kN > V_{Ed} = 206.3\ kN$$

A1.4. Verification of the shear strength in the region of positive bending moment, between the load and the central support

The maximum shear in this region is 206.3 kN, produced when there are two point loads. For this load combination, the positive bending moment is 280.8 kNm. Then, the values a/d and ζ are:
Size effect:
The values of x/d =0.296 and cotθ =1.207 as in the first case.

$$\frac{a}{d} = \frac{M_d}{V_d\, d} = \frac{280.8}{206.3 \cdot 0.5} = 2.72;$$

$$\frac{x}{d} = n\rho_l \left(1 + \sqrt{1 + \frac{2}{n\rho_l}}\right) = 0.282; \qquad x = 141\ mm$$

$$\zeta = \frac{2}{(2.72)^{0.2} \sqrt{1 + \frac{500}{200}}} = 0.87$$

$$V_{cu} = 0.3 \zeta \frac{x}{d} f_{cd}^{2/3} b_{v,eff}\, d = 0.3 \cdot 0.875 \cdot 0.296 \cdot 16.67^{2/3} \cdot 400 \cdot 500 = 101.2 KN < V_{cu,min}$$

The shear reinforcement amount is $\frac{A_{sw}}{s_t} = \frac{100}{200} = 0.5\ \frac{mm^2}{mm^2}$

then the contribution of the stirrups is:

$$V_{su} = 1.4 \frac{A_{sw}}{s} f_{ywd} (d_s - x)\, sin\alpha\, (cot\theta + cot\alpha) = 1.4\ 0.5 \cdot 400 \cdot 0.352 = 119\ kN$$

The total shear resisted is, then
$V_{Rd} = V_{cu} + V_{su} = 101.2 + 119.0 = 220.2$ kN > V_{Ed}=206.3 kN, OK

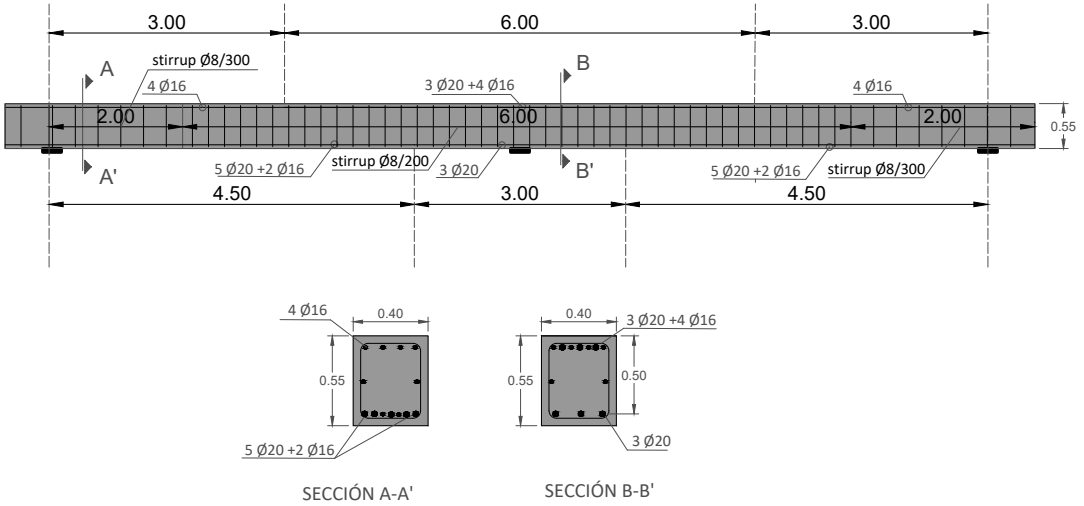

Figure A1.2 Reinforcement arrangement